Dalton Transactions

Accepted Manuscript

ROYAL SOCIETY OF CHEMISTRY

www.rsc.org/dalton

Journal Name

ARTICLE

Received 00th January 20xx,
Accepted 00th January 20xx
DOI: 10.1039/x0xx00000x
www.rsc.org/

Insight into the Stereoelectronic Parameters of N-Triphos Ligands via Coordination to Tungsten(0)

Andreas Phanopoulos, Andrew J. P. White, Nicholas J. Long,* Philip W. Miller*

A series of new N-triphos tungsten complexes have been synthesised and structurally characterised. The coordination behaviour of a range of N-triphos ($N(CH_2PR_2)_3$, NP_3^R) ligands, and a mixed-arm diphosphine-pyridyl (PPN^{Cyh}) ligand were explored. The steric and electronic parameters of five N-triphos ligands: NP_3^{Ph}, NP_3^{iPr}, NP_3^{Cyp}, NP_3^{Cyh} and NP_3^{PhF2}, and the carbon-centred triphos ligand, $CH_3C(CH_2PPh_2)_3$ ($MeCP_3^{Ph}$), were established. Steric parameters were evaluated by analysing the cone angles calculated from X-ray crystal structures, whilst the electron-donating ability of the ligands was determined from ^{31}P-^{77}Se NMR coupling constants of selenium derivatives and the IR carbonyl stretching frequencies across a series of tungsten-carbonyl complexes. In general, electron-rich phosphines formed bidentate complexes while less electron-rich ligands coordinated in a tridentate mode, regardless of steric bulk. An indirect interaction between the apical nitrogen of the ligand and metal centre is implicated for tridentate complexes and is supported through DFT calculations and analysis of N-protonated complexes. Complexes **1**, **3**, **4**, **6**–**8** and **10** were characterised by single-crystal X-ray crystallography.

Introduction

Triphosphosphines have recently re-emerged as excellent ligands for the synthesis of active homogeneous transition metal catalysts for a series of challenging reactions. Notable recent examples of such catalytic transformations using triphos based complexes include the hydrogenation of carboxylic acid derivatives,[1] selective bond cleavage of lignin model compounds,[2] alkylation of amines,[3] amination of alcohols,[4] and the reduction of CO_2 to methanol.[5]

Conventionally, these ligands contain a central apical moiety with three branching phosphino arms that are typically used to enforce well defined tridentate complexes (fig. 1). The stability of these complexes and their tridentate *facial* coordination environment at octahedral metal centres is thought to be key to their success as catalysts. Many variations on triphos ligands have been reported that contain different coordinating groups (phosphines, thiols, imines *etc.*)[6-8] spacer lengths (n = 0, 1, 2 *etc.* fig. 1)[9-12] and various ancillary R-groups (methyl, vinyl, benzyl *etc.*).[13-15] Relative to the carbon-centred $R'CP_3^R$ ligands, variations with heteroatomic apical moieties have not been as extensively studied. In some cases these variations have displayed unique coordination and catalytic chemistry that is a direct result of the heteroatom in the ligand framework.[7] Boron-centred ligands $PhB(CH_2PR_2)_3$, pioneered by the Peters and Tilley groups, have received most attention.[16-18] Recently our group reported a range of nitrogen-centred triphos, $N(CH_2PR_2)_3$ (NP_3^R), ruthenium complexes and explored their catalytic activity for levulinic acid hydrogenation.[19,20] Interestingly, we demonstrated that this ligand motif was capable of performing on par or better than the well known carbon-centred ligands.[20]

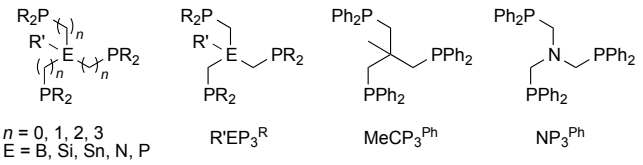

Figure 1 Structure of the triphos ligand scaffold

Branched triphos ligands typically bind to transition metals via all three phosphine arms in a tridentate fashion, however, bidentate coordination is also possible depending on the ligand sterics, choice of metal centre and reaction conditions.[21-22] Changes in denticity *i.e.* the interconversion from κ^2 to κ^3 can have significant consequences for the reactivity of such complexes.[23] As mentioned above, *facial* coordination environment is desirable for catalytic activity and to ensure stability under forcing reaction conditions, hence in order to better design and tune new triphos based catalysts detailed knowledge of their coordination chemistry is needed. The coordination of bidendate phosphine complexes has been very well studied over the past decade in terms of stereo-electronic parameters, and related to their reactivity.

Department of Chemistry, Imperial College London, South Kensington, London, SW7 2AZ, UK.

Electronic Supplementary Information (ESI) available: [details of any supplementary information available should be included here]. See DOI: 10.1039/x0xx00000x

Comparable studies of triphos complexes have, however, not been conducted in detail. Further investigation into the coordination of triphos ligands is therefore warranted considering their recent application in a range of catalytic reactions in order to better understand their bonding characteristics and to optimise reactivity. Previously, it was thought that the steric profile of the phosphines dominated the coordination chemistry of NP_3^R ligands, but recently the electronic characteristics have been shown to be as important,[19] which is explored further in this report.

Herein, we report a series of tungsten(0) complexes featuring a range of NP_3^R ligands, and a "mixed-arm" phosphine-pyridyl derivative. The ligands were conveniently prepared via a phosphorus based Mannich reaction and display a range of stereo-electronic parameters. Tungsten was selected to study the coordination chemistry of these ligands since it forms stable and well-defined octahedral complexes. The presence of the naturally occurring NMR-active W-183 (I = 1/2) isotope enables further spectroscopic analysis.

Results and discussion

Ligand synthesis

Six different ligands were selected for this study that display a range of stereo-electronic parameters (Scheme 1); four have been previously reported by us and others: NP_3^{Ph}, NP_3^{iPr}, NP_3^{Cyp} and NP_3^{Cyh},[19,24-27] while PPN^{Cyh} and NP_3^{PhF2} are new. The ligands were conveniently synthesised via a phosphorus-based Mannich reaction, either using stable phosphonium salts or hydroxymethyl phosphine intermediates that were generated *in situ* (Scheme 1). One of the main advantages of this Mannich based reaction approach is the ease of nitrogen-centred ligand synthesis with different R-groups on phosphorus. Since many secondary phosphines are commercially available, generating a family of these NP_3 ligands with different stereo-electronic properties is more straightforward than comparable carbon-centred ligands whose synthesis typically requires very air- and moisture-sensitive metal phosphide reagents.

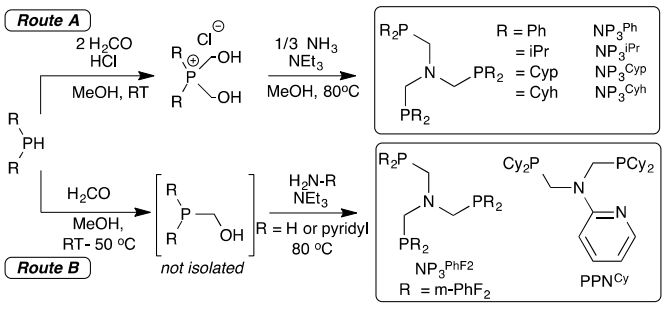

Scheme 1 Synthesis of NP_3^R and PPN^{Cyh} ligands

The known ligands NP_3^{Ph}, NP_3^{iPr}, NP_3^{Cyp} and NP_3^{Cyh} can be conveniently prepared via route A (scheme 1) and isolated as analytically pure samples either simple filtration following precipitation or phase-separation from the crude reaction mixture. The synthesis of the two new ligands PPN^{Cyh} and NP_3^{PhF2} was achieved via route B (scheme 1) starting from the appropriate secondary phosphine and *in situ* generation of the hydroxymethyl phosphines, before undergoing reaction with the relevant amine (Scheme 1). Starting from the phosphonium salts in the case of these ligands gave much lower yields. The work-up procedure for PPN^{Cyh} and NP_3^{PhF2} was not as a simple as the other ligands in this series. PPN^{Cyh} was purified, after solvent and volatiles were removed, by recrystallisation from boiling DMF. The isolated colourless crystals showed a characteristic singlet at –12.2 ppm in the $^{31}P\{^1H\}$ NMR spectrum. NP_3^{PhF2} was isolated as a gummy residue after removal of solvent. Addition of hexane to this residue with stirring resulted in the precipitation of a white powder. Isolation via filtration, washing with cold hexane and drying *in vacuo* gave an analytically pure sample with a $^{31}P\{^1H\}$ NMR signal at –24.8 ppm. The ^1H and ^{13}C NMR spectra, and mass spectra for both PPN^{Cyh} and NP_3^{PhF2} confirmed the ligand structures.

Tungsten Coordination

The coordination chemistry of NP_3^{iPr}, NP_3^{Cyp}, NP_3^{PhF2} and PPN^{Cyh} was evaluated by coordination to tungsten(0) precursors, and compared to that of the parent NP_3^{Ph}. Additionally, the previously reported tungsten complexes of NP_3^{Cyh}, $[W(CO)_4(\kappa^2\text{-}NP_3^{Cyh})]$ (**9**), and $MeCP_3^{Ph}$ $[W(CO)_3(\kappa^3\text{-}MeCP_3^{Ph})]$ (**11**) will be considered to supplement the analysis.[24,28] Tungsten hexacarbonyl was selected to study the complexation as group 6 carbonyls are widely known to react with phosphine ligands *via* carbonyl displacement, and may be anticipated to form facially capping tricarbonyl complexes with NP_3^R ligands. Furthermore, the W-183 isotope is spin-active (abundance ~14%) and enables phosphine coordination to tungsten to be easily recognized by the presence of ^{183}W-satellites in the ^{31}P NMR spectra.

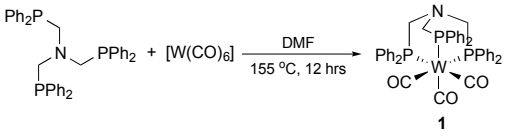

Scheme 2 Tridentate coordination of NP_3^{Ph} to $[W(CO)_6]$

Coordination of NP_3^{Ph} to $[W(CO)_6]$ resulted in formation of the expected tricarbonyl complex $[W(CO)_3(\kappa^3\text{-}NP_3^{Ph})]$ (**1**) with the triphosphine ligand coordinated in a tridentate mode (Scheme 2). Forcing conditions (155 °C, 12 hours) were required to obtain reasonable yields of 1. Under milder conditions (50 °C, four hours) and using the more labile reagent $[W(CO)_4(pip)_2]$ (pip = piperidine), tridentate coordination was still observed, albeit as the minor product compared to the corresponding bidentate complex $[W(CO)_4(\kappa^2\text{-}NP_3^{Ph})]$ (**2**) (Scheme 3). This is evident from the $^{31}P\{^1H\}$ NMR spectrum of the reaction mixture (Figure 2), which indicates a mixture of bidentate species **2** that shows phosphorus resonances at –2.4 ppm and –29.9 ppm, and tridentate species **1** that shows a single phosphorus resonance

at δ: –21.3 ppm. Complex 1 was found to be present in 7% yield compared to **2** in the reaction mixture, based on the relative integrations of the corresponding phosphorus resonance peaks. This is analogous to the coordination behavior displayed by $MeCP_3^{Ph}$ upon coordination to tungsten(0).[22]

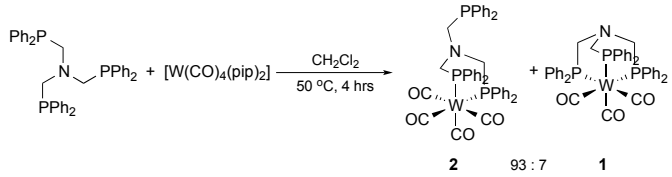

Scheme 3 Predominantly bidentate coordination of NP_3^{Ph} to $[W(CO)_4(pip)_2]$

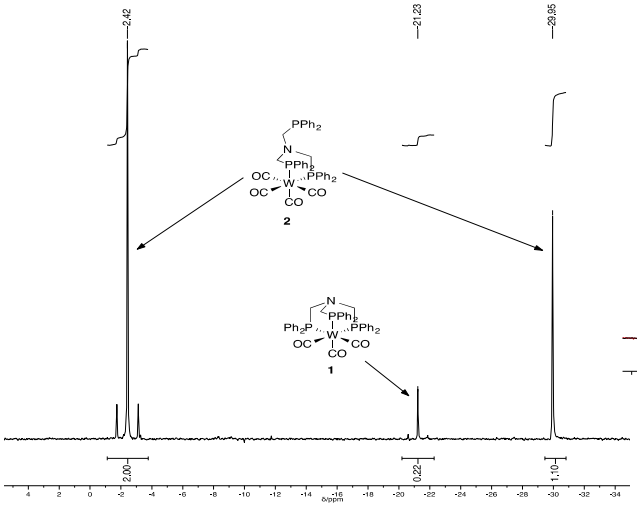

Fig. 2 $^{31}P\{^1H\}$ NMR spectrum of reaction mixture between NP_3^{Ph} and $[W(CO)_4(pip)_2]$ ($CDCl_3$, 162 MHz), showing mixture of κ^3-complex **1** and κ^2-complex **2**

The accessibility of the lone pair on the apical nitrogen of NP_3^{Ph} of complex **1** was investigated by protonation.[29] It was found that strong acids such as HCl (pK_a –0.4 in DCE) and HBF_4 (pK_a –10.3 in DCE)[30] were required to effect protonation. Weaker proton donors such as NH_4PF_6 (pK_a 6.2 in DCE) did not react with **1** even after heating. Stirring a solution of **1** in CH_2Cl_2 with excess 48 wt. % aqueous HBF_4 solution at room temperature resulted in protonation of the apical nitrogen and formation of the cationic complex $[W(CO)_3(\kappa^3\text{-}HNP_3^{Ph})][BF_4]$ (**3**) (Scheme 4).

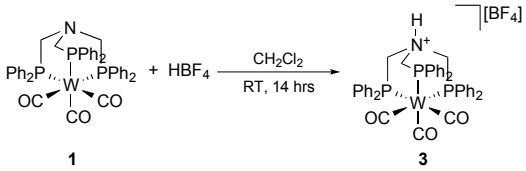

Scheme 4 Protonation of **1** at the apical nitrogen using HBF_4

Spectroscopic characterisation of **3** suggests that electron density has been removed from the tungsten centre relative to **1**. This is evident from the downfield shift of 11.3 ppm in the phosphorus resonance by $^{31}P\{^1H\}$ NMR spectroscopy (Figure 3) and the shift to higher wavenumbers of carbonyl stretching frequencies in the IR spectrum (Figure 4). The net removal of electron density from tungsten may be due to the proximity of the metal centre to the newly generated positive charge at nitrogen upon protonation. Indeed, electrostatic arguments may account for the observed spectroscopic differences between **1** and **3**. Alternatively, as was suggested by Huttner,[29] an interaction between the apical nitrogen and tungsten atoms may exist, and protonation of the nitrogen results in removing the contribution made to this interaction by the nitrogen lone pair. This interaction cannot be a formal bond as the two atoms are separated by a distance of over 3.5 Å (*vide infra*) and a hexa-coordinated tungsten(0) complex does not have unoccupied bonding orbitals to accept the nitrogen lone pair.

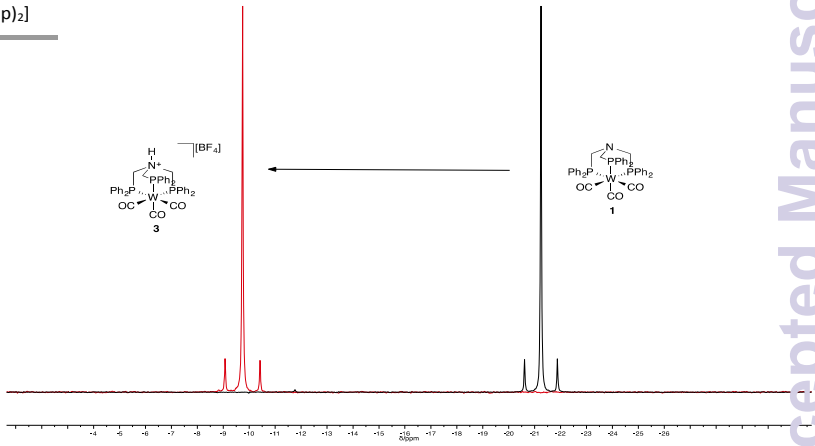

Fig. 3 The downfield shift in phosphorus resonance by $^{31}P\{^1H\}$ NMR spectroscopy upon protonation of **1** (CD_2Cl_2, 162 MHz)

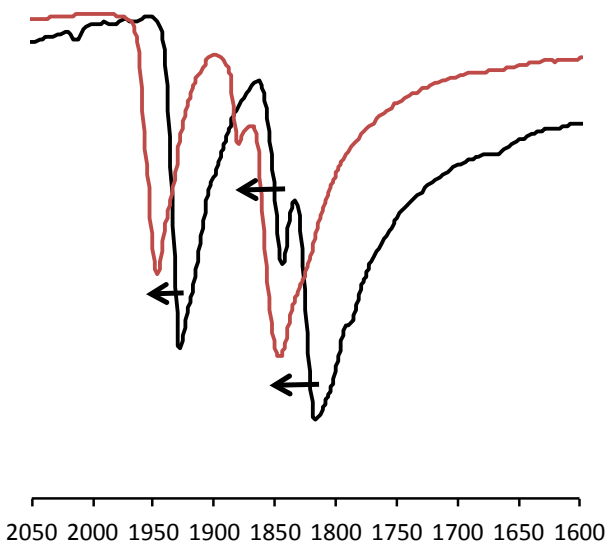

Fig. 4 The shift in carbonyl stretching frequencies (cm^{-1}) by infra-red spectroscopy upon protonation of **1**

NP_3^{PhF2}, which features *meta*-difluorophenyl substituents at phosphorus, was found to coordinate to tungsten(0) in a similar fashion to NP_3^{Ph}. Reaction of NP_3^{PhF2} with $[W(CO)_6]$ at 155 °C for 13 hours exclusively gave the tridentate complex $[W(CO)_3(\kappa^3\text{-}NP_3^{PhF2})]$ (**4**). Reaction of NP_3^{PhF2} under milder conditions (55 °C, five hours, $[W(CO)_4(pip)_2]$) gave a mixture of

bi- and tridentate complexes, $[W(CO)_4(\kappa^2\text{-}NP_3^{PhF2})]$ (**5**) and **4**, respectively, in a ratio of 22:3 (**5**:**4**). The similarity in reactivity between NP_3^{Ph} and NP_3^{PhF2} was surprising given the increased steric demand of NP_3^{PhF2} (*vide infra*), as previous reports had suggested that coordination of NP_3^{R} ligands was controlled by the steric requirements of the ligand.[24]

Ligands NP_3^{iPr} and NP_3^{Cyp} with alkyl substituents displayed different coordination chemistry exclusively forming bidentate complexes **6** and **7** (Scheme 5). Attempts to convert these complexes to the corresponding tridentate analogues *via* by heating in high-boiling solvents such as propylene carbonate (b.p. 242 °C), decaline (b.p. 187–196 °C) or DMSO (b.p. 189 °C) were unsuccessful. Only trace amounts of the desired complexes were detected, with a significant amount of decomposition to 'tungsten black'.

In a typical experiment, the solution or suspension of the tungsten complex was heated to 150 °C for two hours and analyzed by $^{31}P\{^1H\}$ NMR spectroscopy. At this stage the reaction mixture would contain predominantly the bidentate starting material, and small amounts of tridentate complex or another bidentate species whose pendant phosphine arm had undergone oxidation. An approximate ratio of 1:3:12 (κ^3-complex:κ^2-complex with oxidised pendant arm:κ^2-complex) was observed (Figure 5). Continued heating at temperatures between 100–195 °C resulted in either complete decomposition of the complexes to 'tungsten black' or conversion to the previously mentioned κ^2-complex with oxidised pendant arm. When **7** was heated in DMSO for 38 hours between 100–150 °C, the bidentate species $[W(CO)_4(\kappa^2P\text{-}\{N(CH_2PCyp_2)_2(CH_2P(O)Cyp_2)\})]$ (**8**) was isolated and no traces of the desired tridentate complex were detected (Scheme 5).

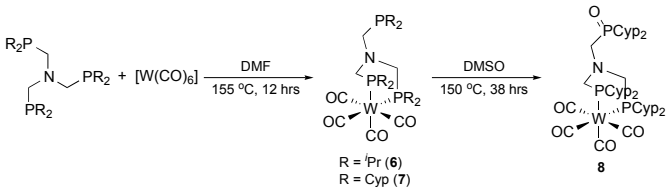

Scheme 5 Exclusive bidentate coordination of NP_3^{iPr} and NP_3^{Cyp} to $[W(CO)_6]$.

The previously reported bidentate tungsten(0) carbonyl complex of NP_3^{Cyh} $[W(CO)_4(\kappa^2\text{-}NP_3^{Cyh})]$ (**9**) could not be converted to the tridentate analogue.[24] Consequently, the mixed arm ligand PPN^{Cyh} was investigated as replacement of one bulky dicyclohexyl arm with a potentially sterically smaller pyridyl group may intuitively allow tridentate coordination. Unfortunately, upon reaction of PPN^{Cyh} with $[W(CO)_6]$, only the bidentate species $[W(CO)_4(\kappa^2P\text{-}PPN^{Cyh})]$ (**10**) was isolated, which features PPN^{Cyh} coordinating through both phosphine arms, leaving the pyridyl group pendant. Attempts to force CO displacement and pyridyl coordination by heating crystals of **10** in a sealed ampule under static vacuum at 150 °C for 23 hours failed. Qualitatively, a black powder was observed after heating (presumably 'tungsten black' from decomposition) and NMR spectroscopic analysis of the remaining pale yellow crystals only showed starting material. It appears heating under vacuum results only in decomposition without chelation of the pyridyl group. Additionally, irradiation with UV light using a mercury lamp in an attempt to eject a CO ligand and enable coordination was also unsuccessful.

These observations qualitatively suggest that the steric encumbrance of the ligands is not solely controlling the coordination behaviour of NP_3^{R} ligands but rather it is the more electron-donating phosphines that preclude coordination of all three arms.

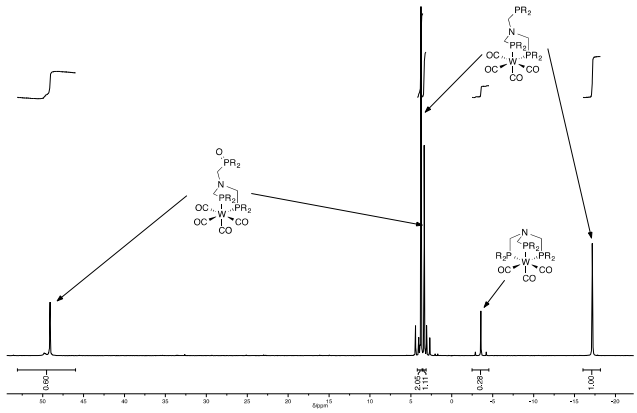

Fig. 5 Representative $^{31}P\{^1H\}$ NMR spectrum of reaction mixture after heating either **6** or **7** in DMSO at 150 °C for two hours (d_6-DMSO, 162 MHz, 100 °C), showing mixture of κ^3-complex, κ^2-complex with oxidised pendant phosphine and κ^2-complex.

Crystal Structures

Crystals of complexes **1**, **3**, **4**, **6**–**8** and **10** suitable for X-ray diffraction experiments were grown (Figure 6 for **1**, **3** and **4** and Figure 7 for **6A, 7** and **10A;** Supplementary Information for **4'**, **6B**, **8** and **10B**). Complexes **6** and **10** crystallised as two crystallographically independent complexes (**6A**, **6B**, **10A** and **10B**). Two separate samples of complex **4** were analysed by X-ray diffraction experiments, and were found to crystallise in separate space groups (**4** and **4'**). Crystals grown from the synthesis of **4** starting from NP_3^{PhF2} and $[W(CO)_6]$, and recrystallised from boiling $CHCl_3$, crystallised in the monoclinic $P2_1/n$ space group (Figure 6). The second crystal sample was grown directly from a reaction solution after attempts to methylate the apical nitrogen in a sample of **4** using Me_3OBF_4 were unsuccessful. These were crystallised by layering diethyl ether onto a concentrated CD_2Cl_2 solution containing both **4** and Me_3OBF_4, and were found to crystallise in the triclinic $P\bar{1}$ space group (Figure S29).

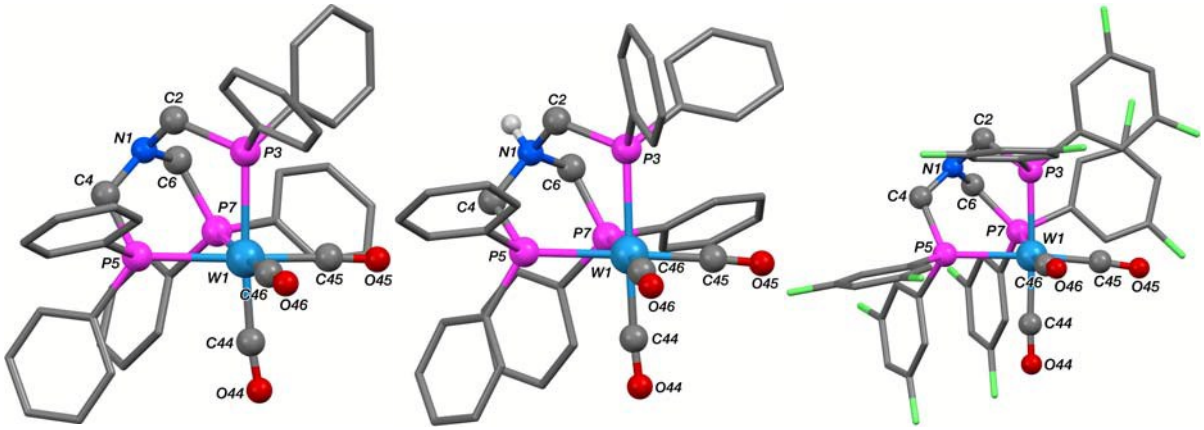

Fig. 6 The crystal structures of **1** (left), **3** (middle) and **4** (space group: $P2_1/n$, right); hydrogens around the phenyl rings and methylene carbons, and BF_4 anion in **3** have been omitted for clarity.

Table 1 Selected bond lengths (Å) and angles (°) for complexes in crystals of **1**, **3** and **4.**

	1	3	4		1	3	4
W(1)–P(3)	2.5148(6)	2.507(3)	2.5038(14)	P(3)–W(1)–C(45)	91.02(8)	94.7(3)	97.11(17)
W(1)–P(5)	2.5354(7)	2.488(3)	2.5059(13)	P(3)–W(1)–C(46)	90.96(8)	95.7(3)	86.67(17)
W(1)–P(7)	2.5131(6)	2.508(3)	2.4961(13)	P(5)–W(1)–C(44)	95.74(8)	94.8(3)	89.49(16)
W(1)–N(1)	3.615(2)	3.657(8)	3.656(5)	P(5)–W(1)–C(45)	175.94(8)	176.5(3)	171.88(16)
W(1)–C(44)	1.982(3)	1.988(10)	1.983(6)	P(5)–W(1)–C(46)	98.95(8)	95.0(3)	101.41(17)
W(1)–C(45)	1.975(3)	1.985(10)	1.987(6)	P(7)–W(1)–C(44)	97.62(8)	93.7(3)	101.08(16)
W(1)–C(46)	1.995(3)	2.003(10)	1.994(5)	P(7)–W(1)–C(45)	94.39(8)	95.4(3)	93.02(16)
				P(7)–W(1)–C(46)	175.53(8)	175.9(3)	170.79(16)
P(3)–W(1)–P(5)	87.93(2)	86.66(9)	88.23(4)	C(44)–W(1)–C(45)	85.44(12)	83.8(4)	85.8(2)
P(3)–W(1)–P(7)	84.62(2)	86.13(8)	84.63(4)	C(44)–W(1)–C(46)	86.76(11)	84.6(4)	87.8(2)
P(5)–W(1)–P(7)	81.60(2)	81.45(8)	81.36(4)	C(45)–W(1)–C(46)	84.99(11)	88.0(4)	85.1(2)
P(3)–W(1)–C(44)	175.94(8)	178.4(3)	173.46(16)				

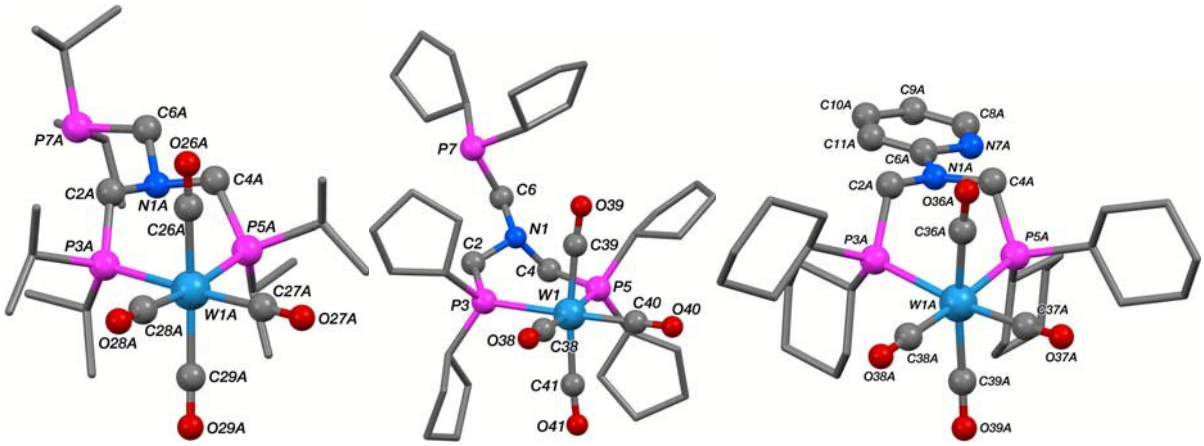

Fig. 7 The crystal structures of **6A** (left), **7** (middle) and **10A** (right) hydrogens around the phenyl rings and alkyl carbons omitted for clarity.

Table 2 Selected bond lengths (Å) and angles (°) for complexes in crystals of **6**, **7** and **10.**

	6A	6B	7	10A	10B		6A	6B	7	10A	10B
W(1)–P(3)	2.529(2)	2.536(2)	2.5269(9)	2.5420(15)	2.5305(19)	P(3)–W(1)–P(5)	82.36(8)	82.33(8)	88.66(3)	84.25(5)	83.75(7)
W(1)–P(5)	2.548(3)	2.548(3)	2.5283(9)	2.5596(16)	2.559(2)						
W(1)–N(1)	4.101(9)	4.094(10)	3.809(3)	4.002(5)	4.028(6)						

Figure 6 illustrates three of the crystal structures (**1**, **3** and **4**) where the ligands are facially capping. The complexes are six-coordinate tungsten centres with distorted octahedral coordination geometries. The bond lengths and angles for all three crystal structures are within the range expected for octahedral tungsten(0) carbonyl complexes (Tables S2–S9).[22,28] Selected key bond lengths and bond angles for the crystal structures of **1**, **3** and **4** are shown in Table 1. Three bidentate complexes **6A, 7** and **10A** are shown in figure 7, selected key bond lengths and the internal P-W-P angles are shown in Table

Table 3 Summary of Tolman and Mingos cone angles and bite angles for NP_3^R ligands and $MeCP_3^P$

Ligand	No. of Phosphines Analysed	Tolman Cone Angle (°)	Mingos Cone Angle (°)	Bite Angle (°)
NP_3^{Ph}	45	134	130	92
$MeCP_3^{Ph}$	5	133	126	97
NP_3^{PhF2}	9	139	132	95
NP_3^{iPr}	7	141	131	93
NP_3^{Cyp}	20	142	135	96
NP_3^{Cyh}	16	149	135	103

Table 4 Summary of phosphine basicity using carbonyl stretching frequencies (BCO) and $^1J_{PSe}$coupling constants (BSe)

Ligand	ν_{CO} (cm^{-1})	B_{CO}	Normalised B_{CO}	$^1J_{PSe}$ (Hz)	B_{Se}	Normalised B_{Se}
NP_3^{PhF2}	1937	0.000516	1.00	755	0.00132	1.00
NP_3^{Ph}	1930	0.000518	1.00	718	0.00139	1.05
$MeCP_3^{Ph}$	1915	0.000522	1.01	714	0.00140	1.06
NP_3^{iPr}	1894	0.000528	1.02	685	0.00146	1.10
NP_3^{Cyp}	1887	0.000530	1.03	683	0.00146	1.11
NP_3^{Cyh}	1878	0.000532	1.03	679	0.00147	1.11

2. The third arm of these ligands is unable to displace a carbonyl ligand to give the tridentate complexes. The pendant arms are orientated away from the metal centre presumably due to steric interactions and the N-W distances of these bidentate complexes are notably longer than that observed for the tridentate complexes. Full experimental data, bond lengths and angles for all crystallographically characterised complexes can be found in the Supplementary Information.

Closer examination of the W–N distances from the crystal structures of **1** and **3** shows that there is a statistically significant difference between the protonated and non-protonated complexes, up to a 3σ level of confidence. The W–N distance in the non-protonated complex **1** is shorter by 0.042 Å than in the protonated **3**. Although this may be indicative of an N–M interaction within complex **1**, electrostatic arguments also offer a viable explanation for the differences observed in the solid-state. The presence of a positive charge within the ligand framework in **3** could significantly alter molecular packing and hence interatomic distances. The average C–O bond distance in the carbonyl ligands of the two crystal structures is also different, however this difference cannot be described to the same level of confidence as the W–N distance.

Discussion

Steric Parameters

The steric parameters of ligands NP_3^{Ph}, NP_3^{PhF2}, NP_3^{iPr}, NP_3^{Cyp} and NP_3^{Cyh}, as well as $MeCP_3^{Ph}$ were evaluated through analysis of the cone angles formed when these ligands coordinate to metal centres, using both published crystal structures and those obtained during the work described herein.[22,24,27-29,31] In total, 41 unique crystal structures containing either κ^2- or κ^3-coordinated NP_3^R ligands were analysed and their cone angles calculated using both the Tolman[32] and Mingos[33] methods (for full details see Supporting Information). Table 3 summarises the calculated values and, similar to other phosphine ligands, the crystallographically calculated cone angles were found to be smaller than those predicted by the Tolman cone angle.[34] The calculated bite angles (average P-M-P angle) are also provided however show no trend. Prior to undertaking these calculations, each M–P bond length in each crystal structure was normalised to 2.28 Å for consistency and comparative purposes to previously reported phosphine cone angles.[32]

The Mingos cone angles will primarily be considered, as these give the best description of the overall steric properties of the ligands across different coordination geometries and environments, as well as coordination to different metal centres. The calculated values show that the steric bulk increases in the order $MeCP_3^{Ph}$ < NP_3^{Ph} < NP_3^{iPr} < NP_3^{PhF2} < NP_3^{Cyp} ≈ NP_3^{Cyh}. This order is as expected except for the similarity in the steric properties of NP_3^{Cyp} and NP_3^{Cyh}; the latter cyclohexyl based ligand proving to be less sterically encumbered as might be expected based on simple intuition.

Electronic Parameters

Two different methods were used to assess the electronic parameters of ligands NP_3^{Ph}, NP_3^{PhF2}, NP_3^{iPr}, NP_3^{Cyp}, NP_3^{Cyh}, and $MeCP_3^{Ph}$. Firstly, the traditional indicator of phosphine electron-donating ability using carbonyl stretching frequencies across a series of carbonyl complexes was evaluated (in this case tungsten). Secondly, the magnitude of the phosphorus-selenium coupling constants for the corresponding phosphine selenides was also assessed.[35,36] Unfortunately, no discernable pattern was observed in ^{31}P NMR chemical shift or $^1J_{P183W}$-coupling constants, so these are not considered in the discussion.

The carbonyl stretching frequencies for six tetracarbonyl tungsten complexes including the triphosphine ligands in a bidentate coordination mode, $[W(CO)_4(\kappa^2\text{-}R'P_3^R)]$, were considered. Four complexes, where $R'P_3^R$ = NP_3^{Ph} (**2**), NP_3^{PhF2}

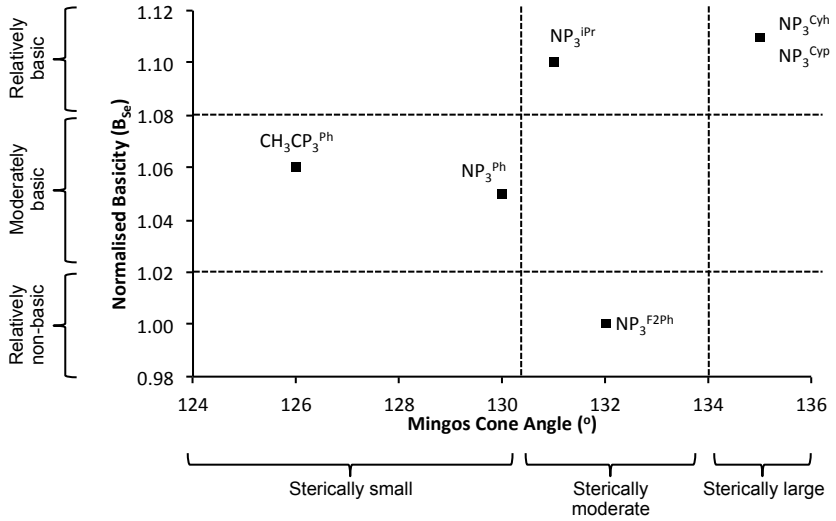

Fig. 8 Plot of steric and electronic parameters of NP_3^R ligands and $MeCP_3^{Ph}$ using calculated Mingos cone angles and phosphorus lone pair basicity based on phosphorus-selenium *J*-coupling constants

(**5**), NP_3^{iPr} (**6**) and NP_3^{Cyp} (**7**) are reported in this work (*vide supra*); while the remaining two complexes where $R'P_3^R$ = NP_3^{Cyh} (**9**) and MeP_3^{Ph} (**12**) are reported elsewhere.[22,24] In each case the symmetrical CO stretching frequency (ν_{CO}) was identified, allowing basicity to be determined from the reciprocal of ν_{CO} ($1/\nu_{CO} = B_{CO}$).

The phosphine selenides were prepared by shaking a solution of the desired ligand in $CDCl_3$ with an excess of elemental selenium and filtering through a small pad of celite. The $^1J_{PSe}$-coupling constant was determined by $^{31}P\{^1H\}$ NMR spectroscopy and the basicity determined from its reciprocal ($1/^1J_{PSe} = B_{Se}$). Table 4 summarises the absolute values for ν_{CO}, B_{CO}, $^1J_{PSe}$ and B_{Se}, as well as the normalised basicity values for ease of comparison.

By comparing the normalised B_{CO} and B_{Se} values, it can be observed that both quantification systems show the same overall trend, *i.e.* the ligands can be arranged NP_3^{PhF2} < NP_3^{Ph} < $MeCP_3^{Ph}$ < NP_3^{iPr} < NP_3^{Cyp} ≈ NP_3^{Cyh} from least to most basic. One difference to note is that the B_{CO} values predict the basicity of the phosphorus lone pairs to be relative similar, since the normalised B_{CO} vales have a range of only 0.03, while the normalised B_{Se} values range over 0.11. From experimental observations, ligands NP_3^{iPr}, NP_3^{Cyp} and NP_3^{Cyh} have coordination chemistry that differs from NP_3^{Ph} and NP_3^{PhF2}; this is not likely to be sterically controlled. Therefore it appears that B_{Se} more reliably describes the lone pair basicity of NP_3^R ligands as it shows a more pronounced change (ΔB_{Se}[**5**–**6**] = 0.05) in basicity between the two groups of ligands, compared to B_{CO} (ΔB_{CO}[**5**–**6**] = 0.02).

A plot of Mingos cone angles against B_{Se} (Figure 8) allows the evaluation of both the steric and electronic parameters of the NP_3^R ligands (and $MeCP_3^{Ph}$ for comparison). As might be expected there is no trend between the steric and electronic properties, but the ligands can be grouped into three sets based on their steric encumbrance: small (NP_3^{Ph} and $MeCP_3^{Ph}$), moderate (NP_3^{iPr} and NP_3^{PhF2}) and large (NP_3^{Cyp} and NP_3^{Cyh}). Within these sets, the sterically smallest and largest ligands also have similar electron-donation abilities, however the moderately bulky ligands have distinctly different phosphine lone pair donating abilities with NP_3^{PhF2} being significantly less Lewis basic than NP_3^{iPr}. Comparing the coordination behaviour of NP_3^{iPr} and NP_3^{PhF2} with $[W(CO)_6]$ (*vide supra*) illustrates the significance of phosphine basicity in the ability for all three phosphine moieties to coordinate to a metal centre. Namely, more electron-donating NP_3^R ligands are less likely to coordinate in a tridentate mode in tungsten(0) carbonyl complexes.

A comparative study between the coordination of NP_3^{Ph} and NP_3^{Cyp} to ruthenium precursors revealed similar electronic control.[25] Relatively less basic NP_3^{Ph} was found to coordinate to both ruthenium(0) and ruthenium(II) in a tridentate coordination mode. On the other hand, the more basic NP_3^{Cyp} only coordinated to ruthenium(II) through all three phosphine donors, while coordinating in a bidentate mode to electron-rich ruthenium(0) precursors.

Density Functional Theory Analysis

Experimental observations in conjunction with calculated ligand steric and electronic properties suggest that tridentate coordination of NP_3^R ligands is not sterically controlled, but rather, determined by the overall electronics of the complex. Additionally, protonation of the apical nitrogen of NP_3^{Ph} in complex **1** and subsequent spectroscopic characterisation suggests some electronic communication exists between the nitrogen and metal centre. A similar argument was proposed for the corresponding molybdenum complex.[29] To gain further insight into the electronic nature of $[W(CO)_x(EP_3^R)]$ type complexes, density functional theory calculations were performed on nine different complexes featuring both bidentate and tridentate coordination modes, and with both carbon- and nitrogen-centred triphosphines. The reported complexes **1**–**3**, **7** and **11** were evaluated along with the theoretical complexes $[W(CO)_3(\kappa^3\text{-}NP_3^{Cyp})]$ (**13**), $[W(CO)_3(\kappa^3$-

HNP_3^{Cyp})]$^+$ (**14**), [W(CO)$_4$(κ^2-$MeCP_3^{Cyp}$)] (**15**) and [W(CO)$_3$(κ^3-$MeCP_3^{Cyp}$)] (**16**) (Figure 9).

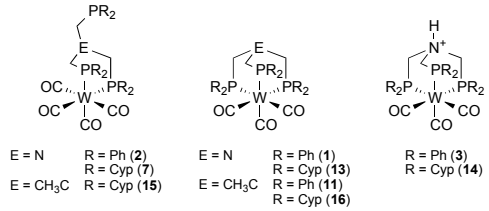

Fig. 9 Complexes studied using density functional theory calculations

Crystal structures obtained from single crystals X-ray diffraction experiments of complexes **1**, **3**, **7** and **11**[29] were used as starting points for the calculations. Each structure was first optimised using B3LYP as the functional, MWB60 as the basis set and pseudo-potential for tungsten and 6-31G* as the basis set for all other atoms.

Visualisation of the HOMOs for complexes **1**–**3**, **7**, **11** and **13**–**16** shows apparent overlap of nitrogen and metal based orbitals, that originate from atomic orbitals of *p* and d_{z^2} parentage, respectively. This can be seen in Figure 10 as a continuous channel of electron density that connects the tungsten and nitrogen atoms in complexes **1** and **13**. This interaction is lost upon changing the coordination mode to bidentate (Figure 11A), protonation of the nitrogen (Figure 11B) or substitution of the nitrogen with carbon (Figure 11C).

The nature of the N–W interaction was assessed by natural bond order (NBO) analysis which suggests, as expected, no *classical* bond exists between the two atoms. This is reasonable considering the interatomic distance is >3.5 Å, which is much larger than the sum for both covalent radii (2.05 Å).[37] Despite no formal bond between nitrogen and tungsten, NBO analysis provides insight into the nature of other bonds within the complex that might affect the proposed N–W interaction. Firstly, the W–P bonds were considered, and evaluation of the atomic based orbitals from each atom that contribute to the bond show that the tungsten's contributing hybrid orbital mainly consists of *p*-character (52.58%), rather than *d*-character (32.59%) as might be expected. This suggests there is considerable *d*-*p* mixing on tungsten, which may explain how the metal is able to accept additional electron density; formally increasing its electron count beyond an 18-electron complex. Secondly, the second order perturbation theory analysis was considered for each complex. For complexes **1** and **13** this analysis shows that in both cases, the nitrogen lone pair is primarily interacting with each of the three flanking C–P σ* bonds from the triphosphine ligand scaffold uniformly (Figure 12). These interactions are supported from crystallographic data, but as previously mentioned, can also be explained using electrostatic arguments.

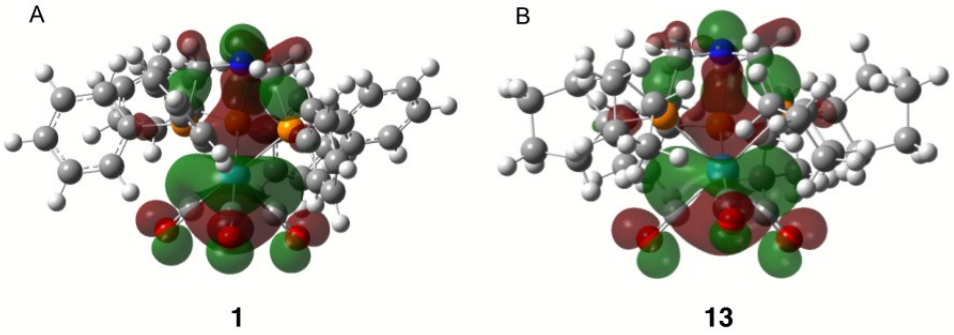

Fig. 10 Contour map of HOMOs for complexes (A) [W(CO)$_3$(κ^3-NP_3^{Ph})] (**1**) and (B) [W(CO)$_3$(κ^3-NP_3^{Cyp})] (**13**) showing overlap of nitrogen and tungsten based orbitals

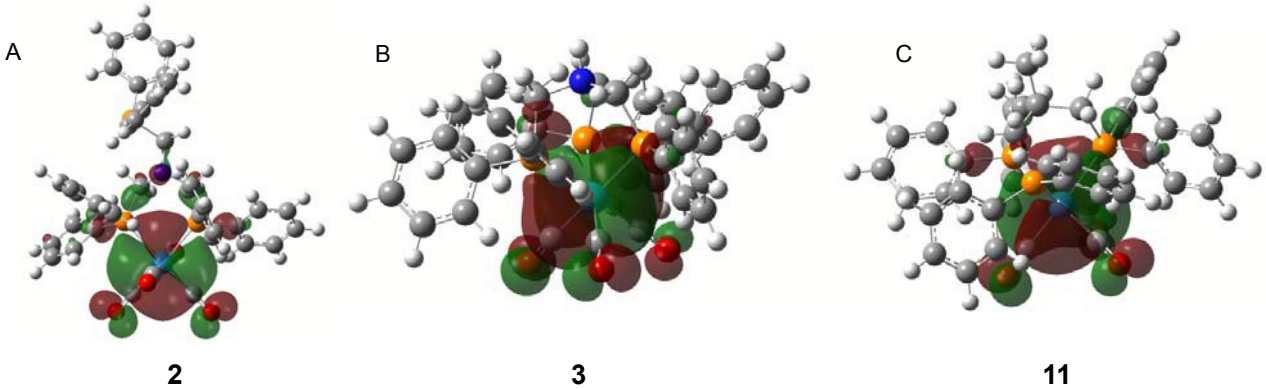

Fig. 11 Contour map of HOMOs for complexes (A) [W(CO)$_4$(κ^2-NP_3^{Ph})] (**2**), (B) [W(CO)$_3$(κ^3-HNP_3^{Ph})]$^+$ (**3**) and (C) [W(CO)$_3$(κ^3-$MeCP_3^{Ph}$)] (**11**)

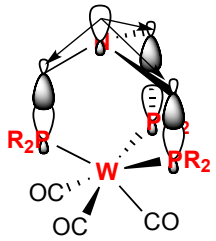

Fig. 12 Proposed significant interactions of nitrogen-centred lone pair with C–P σ* bonds

These interactions may partially explain the apparent electronic communication between the nitrogen and tungsten atoms. If the nitrogen lone pair is delocalised into the flanking C–P σ* bonds, then the metal will be less able to back donate to phosphorus, as the C–P σ* bonds are use as π-acceptor orbitals. Upon protonation of the apical nitrogen, the N → C–P σ* interaction is severed, strengthening the C–P σ bond. This will increase the basicity of the phosphine lone pair which will now be able to coordinate more strongly to tungsten *via* a stronger σ donation. This increase in basicity will be observed spectroscopically as a downfield shift in the $^{31}P\{^{1}H\}$ NMR spectrum. Furthermore, as the N → C–P σ* interaction was prohibiting tungsten–phosphorus backbonding, protonation of nitrogen would result in increased back donation to phosphorus, in tandem reducing back donation to the carbonyl ligands, accounting for the observed shift in carbonyl stretching frequency observed. Therefore it appears that the apparent N–W interaction is not due to direct orbital overlap, but rather mediated *via* modulating the nitrogen interaction with the three flanking C–P bonds of the NP_3 ligand scaffold.

The DFT analysis, however, has some caveats which preclude the complete and accurate description of interatomic interactions in these complexes. Approximations made during NBO analysis, and the use of pseudo-potentials during optimisation may have lead to over-simplification. Consequently, other more appropriate methods such as the Quantum Theory of Atoms in Molecules (QTAIM) analysis are currently under investigation to further elucidate the observed bonding behavior.

Conclusions

A series of novel nitrogen-centred NP_3-tungsten complexes have been prepared and analysed for their steric and electronic properties. The coordination of these NP_3 ligands, and PPN^{Cyh}, to tungsten(0) precursors revealed unexpected coordination behavior. The coordination behavior of NP_3^{R} ligands is not solely dictated by their steric properties, as previously thought, but rather the electronic contribution plays a dominant role in coordination to the metal. Less electron-donating diaryl phosphines were found to coordinate in a tridentate fashion, while more electron-donating dialkyl phosphines predominantly formed bidentate species.

Analysis of the steric and electronic parameters of the NP_3^{R} ligands *via* several different methods enabled the quantification of these physical attributes. Average cone angles for the ligands were calculated using crystallographic data obtained from 41 unique crystal structures in conjunction with an algorithm proposed by Mingos and co-workers.[33] The Lewis basicity of the phosphorus lone pair was assessed using P-Se coupling constants. It was necessary to obtain ligands with similar steric parameters, but different electron-donating abilities. Ligands of similarly moderate steric encumbrance, NP_3^{iPr} and NP_3^{PhF2}, were found to have considerably different electron-donation abilities suggesting that the different coordination behavior observed can be attributed to electronic differences.

Protonation of the apical nitrogen in the tridentate complex $[W(CO)_3(\kappa^3\text{-}NP_3^{Ph})]$ (**1**) resulted in significant changes to both the IR and $^{31}P\{^{1}H\}$ NMR spectra, suggesting some electronic communication between the nitrogen and metal centre exists. DFT calculations were used to assess the electronic structure of nine different tungsten complexes featuring triphosphine ligands in both bi- and tridentate coordination geometries, as well as containing either nitrogen- or carbon-centred ligands. The calculations show the nitrogen lone pair is interacting with each flanking C–P σ* bond rather than directly interacting with the tungsten centre, and by affecting this interaction, the electronic characteristics of the metal centre can be modulated. Hence, electron-rich NP_3 ligands will not coordinate through all three phosphines since this inhibits stabilisation of the complex by removal of electron density at the metal centre by back donation.

In general, NP_3^{R} ligands were shown to display interesting coordination chemistry, with factors beyond the simple size of the ligand affecting bonding and reactivity. These observations suggest further investigation of the reactivity of NP_3^{R} ligands is merited as new catalytic avenues may be realised through chemistry uniquely associated with this scaffold. The apical nitrogen, that initially appeared to be innocent, may more directly affect the chemistry of these ligands and contribute to the overall reactivity.

Experimental

All preparations were carried out using standard Schlenk line techniques under an inert atmosphere of N_2 unless otherwise stated. Solvents were dried over standard drying agents and stored over 3 Å molecular sieves. All starting materials were of reagent grade and purchased from either Sigma-Aldrich Chemical Co. or VWR International and used without further purification. Ligands NP_3^{Ph}, NP_3^{iPr}, NP_3^{Cyp}, NP_3^{Cyh} were prepared as previously reported.[19,25-27] Complexes **9**,[19] **11**,[28] and **12**,[22] were previously reported, their spectroscopic and crystallographic data were used to supplement the discussion. ^{1}H, $^{13}C\{^{1}H\}$, and $^{31}P\{^{1}H\}$ NMR spectra were recorded on Bruker AV-400, AV-500, or DRX-400 spectrometers at 21 °C unless otherwise stated. Chemical shifts are reported in ppm using the residual proton impurities in the solvents for ^{1}H NMR spectroscopy, the solvent for $^{13}C\{^{1}H\}$ NMR spectroscopy, and an external H_3PO_4 standard for $^{31}P\{^{1}H\}$ NMR spectroscopy. Pseudo triplets that occur as a result of identical *J* value coupling to two or more chemically nonequivalent nuclei are

assigned as dd or ddd and are recognized by the inclusion of only one or two *J*-coupling values. $^{13}C\{^1H\}$ NMR spectra were assigned with the aid of DEPT-135, HSQC, and HMBC correlation experiments. Mass spectrometry analyses were conducted by the Mass Spectrometry Service, Imperial College London. Infrared spectra were recorded on a Perkin-Elmer Spectrum 100 FT-IR spectrometer. Elemental analyses were carried out by Mr. Stephen Boyer of the School of Human Sciences, London Metropolitan University. X-ray diffraction analyses were carried out by Dr. Andrew White of the Department of Chemistry at Imperial College London. Details of single-crystal X-ray diffraction analysis can be found in the Supporting Information.

N,N,N-tris((di(3,5-difluorophenyl)phosphino)methyl)amine (NP_3^{PhF2})

To a Schlenk flask was added di(3,5-difluorophenyl)phosphine (2.02 g, 7.81 mmol) and methanol (5 mL). Degassed aqueous formaldehyde solution (35 wt %, 0.80 mL, 10.1 mmol) was added, and the solution was stirred for one hour at room temperature and 30 minutes at 50 °C. A methanolic solution of NH_3 (2 M, 1.30 mL, 2.60 mmol) was then added and the temperature raised to 80 °C and stirred for 10 hours. Upon cooling to room temperature the solution became cloudy and a white gum settled at the bottom of the Schlenk flask. The solvent and volatiles were removed *in vacuo* and the resultant gummy residue was treated with hexane (5 mL) and stirred, causing the gum to solidify as a white powder, which was isolated *via* cannula. The powder was washed with hexane (3 x 5 mL) and dried *in vacuo* (1.34 g, 1.61 mmol, 62%). ^1H NMR ($CDCl_3$) δ: 3.69 (d, 6H, $^2J_{HP}$ = 4.9 Hz, NCH_2P), 6.77 (tt, 6H, $^3J_{HF}$ = 8.8 Hz, $^4J_{HH}$ = 2.3 Hz, CH$^{para\text{-}Ph}$). $^{13}C\{^1H\}$ NMR ($CDCl_3$, 101 MHz) δ: 59.2–59.4 (m, NCH_2P), 105.3 (t, $^2J_{CF}$ = 25.1 Hz, CH$^{para\text{-}Ph}$), 115.4–115.9 (m, CH$^{ortho\text{-}Ph}$), 139.8–140.0 (m, CF$^{meta\text{-}Ph}$), 163.0 (dt, $^1J_{CP}$ = 253.7 Hz, $^3J_{CP}$ = 11.1 Hz, C$^{ipso\text{-}Ph}$). $^{31}P\{^1H\}$ NMR ($CDCl_3$, 162 MHz) δ: –24.81 (s). ^{19}F NMR ($CDCl_3$, 376 MHz) δ: –108.1 – –108.2 (m). HRMS (ES): *m/z* calcd. for $C_{39}H_{25}NP_3F_{12}$ ($[M+H]^+$) 828.1008, found 828.1024. Anal. calcd. for $C_{39}H_{24}NP_3F_{12}$ (found): C, 56.61 (56.56); H, 2.92 (2.87); N, 1.69 (1.73).

$N(CH_2PCyh_2)_2(C_5H_4N)$ (PPN^{Cyh})

To a Schlenk flask was added dicyclohexylphosphine (5.00 g, 25.5 mmol) and methanol (8 mL). Degassed aqueous formaldehyde solution (35 wt %, 2.62 mL, 33.1 mmol) was added, and the solution was stirred for two hours at room temperature. Toluene (13 mL) and 2-aminopyridine (1.20 g, 12.8 mmol) were added and the solution stirred under reflux for 20 hours. The solvent and volatiles were removed *in vacuo* and the resultant residue was recrytallised from boiling DMF, affording colourless crystals that were isolated, washed with DMF and dried *in vacuo* (2.09 g, 4.06 mmol, 32%). ^1H NMR ($CDCl_3$, 400 MHz) δ: 1.11–1.83 (m, 44H, Cyh), 4.05 (d, 4H, $^2J_{HP}$ = 1.3 Hz, NCH_2P), 6.44–6.47 (m, 1H, H_D), 6.65 (m, 1H, H_B), 7.37–7.41 (m, 1H, H_C), 8.10–8.12 (m, 1H, H_A). $^{13}C\{^1H\}$ NMR ($CDCl_3$, 101 MHz) δ: 26.5 (s, CH_2^{Cyh}), 27.4 (dd, *J* = 9.2 Hz, *J* = 3.5 Hz, CH_2^{Cyh}), 29.8 (d, *J* = 11.2 Hz, CH_2^{Cyh}), 30.0 (d, *J* = 10.6 Hz, CH_2^{Cyh}), 32.7 (d, *J* = 14.5 Hz, NCH_2P), 107.3 (s, $C_{B/D}$), 111.3 (s, $C_{B/D}$), 136.8 (s, C_C), 147.5 (s, C_A). $^{31}P\{^1H\}$ NMR ($CDCl_3$, 162 MHz) δ: –12.2 (s). HRMS (ES): *m/z* calcd. for $C_{31}H_{53}N_2P_2$ ($[M+H]^+$) 515.3684, found 515.3670.

Preparation of NP_3^R Selenides

To prepare phosphine selenides, a NMR sample of the ligand (~10 mg) was dissolved in $CDCl_3$ (1 mL) and excess elemental selenium was added (3–5 mg). The suspension was shaken at room temperature for several minutes, filtered through a small pad of celite to remove excess selenium and the filtrate analyzed by ^1H and $^{31}P\{^1H\}$ NMR spectroscopy.

$[W(CO)_3(\kappa^3\text{-}NP_3^{Ph})]$ (1)

To a suspension of NP_3^{Ph} (320 mg, 0.523 mmol) in DMF (10 mL) was added $[W(CO)_6]$ (178 mg, 0.506 mmol), and the mixture was stirred at 155 °C for 12 hours. The solution turned dark and homogeneous. The solvent was removed *in vacuo*, affording a grey residue that was treated with boiling $CHCl_3$ (7 mL), filtered and the filtrate layered with methanol (10 mL). Crystals suitable for X-ray diffraction grew overnight and were isolated *via* cannula filtration, washed with methanol (3 x 3 mL) and dried *in vacuo* (180 mg, 0.204 mmol, 39%). ^1H NMR ($CDCl_3$, 400 MHz) δ: 4.03 (s, 6H, NCH_2P), 7.06–7.14 (m, 12H, CH^{Ph}), 7.16–7.23 (m, 6H, CH^{Ph}), 7.23–7.32 (m, 12H, CH^{Ph}). $^{13}C\{^1H\}$ NMR ($CDCl_3$, 101 MHz) δ: 53.8 (s, NCH_2P), 128.3 (s, CH^{Ph}), 129.1 (s, CH^{Ph}), 132.1 (q, J_{CP} = 3.6 Hz, CH^{Ph}), 137.8 (s, CH$^{ipso\text{-}Ph}$), 211.9 (s, CO). $^{31}P\{^1H\}$ NMR ($CDCl_3$, 162 MHz) δ: –21.3 (s) with ^{183}W satellites (d, $^1J_{P183W}$ = 205.3 Hz). ATR-FTIR (ν/cm^{-1}): carbonyl stretches 1816, 1844, 1928. HRMS (ES): *m/z* calcd. for $C_{42}H_{37}NO_3P_3{}^{184}W$ ($[M+H]^+$) 880.1496, found 880.1481. Anal. calcd. for $C_{42}H_{36}NO_3P_3W$ (found): C, 57.36 (57.27); H, 4.13 (4.19); N, 1.59 (1.58).

$[W(CO)_4(\kappa^2\text{-}NP_3^{Ph})]$ (2)

To a solution of NP_3^{Ph} (433 mg, 0.709 mmol) in CH_2Cl_2 (25 mL) was added $[W(CO)_4(pip)_2]$ (330 mg, 0.708 mmol), and the solution stirred at 50 °C for four hours. After cooling to room temperature the solution was concentrated to ~5 mL, diluted with methanol (20 mL) and concentrated to half the original volume, causing precipitation. A further portion of methanol (10 mL) was added to fully precipitate the product as an off-white powder. The powder was isolated *via* cannula filtration, washed with methanol (5 mL) and dried *in vacuo*. The product was recrystallised by layering methanol (5 mL) over a $CHCl_3$ solution (3 mL) and allowing to sit at room temperature overnight. The colourless crystals that grew were isolated, washed with methanol (3 mL) and dried *in vacuo* (187 mg, 0.206 mmol, 29%). ^1H NMR ($CDCl_3$, 400 MHz) δ: 3.50 (d, 2H, $^2J_{HP}$ = 2.5 Hz, NCH_2P), 3.66 (s, 4H, NCH_2P), 7.23–7.57 (m, 30H, Ph). $^{13}C\{^1H\}$ NMR ($CDCl_3$, 126 MHz) δ: 62.0–62.6 (m, NCH_2P-coordinated), 68.4–68.6 (m, NCH_2P-uncoordinated), 128.3 (t, J_{CP} = 4.6 Hz, CH^{Ph}), 128.9 (d, J_{CP} = 6.8 Hz, CH^{Ph}), 129.2 (s, CH^{Ph}), 129.9 (s, CH^{Ph}), 132.6 (t, J_{CP} = 5.3 Hz, CH^{Ph}), 133.2 (s, CH^{Ph}), 133.3 (s, CH^{Ph}), 136.7–137.2 (m, C^{Ph}), 201.8 (t, $^2J_{CP}$ = 7.1 Hz, CO). $^{31}P\{^1H\}$ NMR ($CDCl_3$, 162 MHz) δ: –29.9 (s, P-uncoordinated), –2.42 (s, 2P, P-coordinated) with ^{183}W

satellites (d, $^{1}J_{P183W}$ = 224.0 Hz). ATR-FTIR (v/cm^{-1}): carbonyl stretches 1865, 1881, 1930, 2022. HRMS (ES): *m/z* calcd. for $C_{43}H_{37}NO_4P_3{}^{184}W$ ([M+H]$^+$) 908.1445, found 908.1555. Anal. calcd. for $C_{43}H_{36}NO_4P_3W$ (found): C, 51.91 (51.82); H, 4.00 (4.15); N, 1.54 (1.60).

[W(CO)$_3$(κ^3-HNP$_3^{Ph}$)][BF$_4$] (3)

To a solution of **1** (246 mg, 0.279 mmol) in CH_2Cl_2 (10 mL) was added an aqueous HBF_4 solution (48 wt %, 2.5 mL, 19.1 mmol) and the solution was stirred at room temperature for 14 hours. The solvent was removed *in vacuo* and resultant powder was washed with diethyl ether (3 x 5 mL), partially dissolved in CH_2Cl_2 (15 mL), filtered, and the filtrate layered with diethyl ether (15 mL). Colourless crystals suitable for X-ray diffraction grew overnight, which were isolated, washed with diethyl ether (3 x 5 mL) and dried *in vacuo* (174 mg, 0.180 mmol, 64%). ^{1}H NMR (CD_2Cl_2) δ: 4.22 (s, 6H, NC*H*$_2$P), 7.12–7.23 (m, 12H, CH^{Ph}), 7.23–7.36 (m, 18H, CH^{Ph}). ^{13}C{^{1}H} NMR (CD_2Cl_2, 101 MHz) δ: 51.7–52.2 (m, N*C*H$_2$P), 129.5 (m, CH^{Ph}), 131.0 (s, CH$^{para\text{-}Ph}$), 131.9 (m, CH^{Ph}), 134.6–135.0 (m, CH$^{ortho\text{-}Ph}$), 209.6–209.8 (m, CO). ^{31}P{^{1}H} NMR (CD_2Cl_2, 162 MHz) δ: –10.0 (s) with ^{183}W satellites (d, $^{1}J_{P183W}$ = 219.6 Hz). ^{19}F NMR (CD_2Cl_2, 376 MHz) δ: –150.6 (s, BF_4). ATR-FTIR (v/cm^{-1}): carbonyl stretches 1846, 1880, 1947; CH bends 3061, 3129. HRMS (ES): *m/z* calcd. for $C_{42}H_{37}NO_3P_3{}^{184}W$ ([M–BF_4]$^+$) 880.1496, found 880.1513. Anal. calcd. for $C_{42}H_{37}NO_3BF_4P_3W$ (found): C, 52.15 (52.07); H, 3.86 (3.93); N, 1.45 (1.50).

[W(CO)$_3$(κ^3-NP$_3^{PhF2}$)] (4)

To a suspension of NP$_3^{PhF2}$ in DMF (5 mL) was added [W(CO)$_6$] (301 mg, 0.363 mmol), and the solution slowly heated to 155 °C (heating too rapidly causes [W(CO)$_6$] to sublime) and stirred at this temperature for 13 hours. After allowing to cool to room temperature the solvent was removed *in vacuo* to afford a pale yellow powder that was partially dissolved in CH_2Cl_2 (5 mL), filtered, and the remaining powder was washed with a further 1 mL CH_2Cl_2. The combined filtrate and washings were taken to dryness *in vacuo*, and the resultant powder was recrystallised from boiling $CHCl_3$, affording off-white crystals suitable for X-ray diffraction that were isolated, washed with methanol (2 x 3 mL) and dried *in vacuo* (142 mg, 0.129 mmol, 36%). ^{1}H NMR ($CDCl_3$, 400 MHz) δ: 4.01 (s, 6H, NC*H*$_2$P), 6.64–6.73 (m, 12H, CH$^{ortho\text{-}Ph}$), 6.77 (tt, 6H, $^{3}J_{HF}$ = 8.4 Hz, $^{4}J_{HH}$ = 1.9 Hz, CH$^{para\text{-}Ph}$). ^{13}C{^{1}H} NMR ($CDCl_3$, 101 MHz) δ: 55.1 (m, N*C*H$_2$P), 106.0 (t, $^{2}J_{CF}$ = 25.2 Hz, CH$^{para\text{-}Ph}$), 114.6 (dm, $^{2}J_{CP}$ = 18.7 Hz, CH$^{ortho\text{-}Ph}$), 140.4–141.1 (m, CF$^{meta\text{-}Ph}$), 162.8 (dm, $^{1}J_{CP}$ = 254.9 Hz, CH$^{ipso\text{-}Ph}$), 208.9–209.3 (m, CO). ^{31}P{^{1}H} NMR ($CDCl_3$, 162 MHz) δ: 17.8 (s) with ^{183}W satellites (d, $^{1}J_{P183W}$ = 215.4 Hz). ^{19}F NMR ($CDCl_3$, 376 MHz) δ: –106.2 (t, $^{3}J_{FH}$ = 7.1 Hz, CF^{Ph}). ATR-FTIR (v/cm^{-1}): carbonyl stretches 1840, 1923. HRMS (ES): *m/z* calcd. for $C_{42}H_{25}NO_3F_{12}P_3{}^{184}W$ ([M+H]$^+$) 1096.0365, found 1096.0339. Anal. calcd. for $C_{42}H_{24}NO_3F_{12}P_3W$ (found): C, 46.05 (45.98); H, 2.21 (2.18); N, 1.28 (1.35).

[W(CO)$_4$(κ^2-NP$_3^{PhF2}$)] (5)

To a solution of NP$_3^{PhF2}$ (201 mg, 0.243 mmol) in CH_2Cl_2 (15 mL) was added [W(CO)$_4$(pip)$_2$] (113 mg, 0.242 mmol) and the mixture stirred at 55 °C for five hours. Attempts to purify the resultant product mixture by crystallisation failed, producing only crystals of **5**. Attempts to purify by column chromatography also failed. ^{31}P{^{1}H} NMR ($CDCl_3$, 162 MHz) δ: –26.1 (s), 3.39 (s) with ^{183}W satellites (d, $^{1}J_{P183W}$ = 235.2 Hz).

[W(CO)$_4$(κ^2-NP$_3^{iPr}$)] (6)

To a solution of NP$_3^{iPr}$ (810 mg, 1.99 mmol) in DMF (5 mL) was added [W(CO)$_6$] (700 mg, 1.99 mmol) and the solution heated to 100 °C for two hours. The solvent was removed *in vacuo* and the resultant yellow residue dissolved in $CHCl_3$ (0.5 mL) and layered with methanol (3 mL). White crystals suitable for X-ray diffraction grew overnight, which were isolated, washed with methanol (3 x 2 mL) and dried *in vacuo* (367 mg, 0.538 mmol, 27%). ^{1}H NMR ($CDCl_3$, 500 MHz) δ: 1.05–1.11 (m, 12H, CH$_3^{iPr}$), 1.19–1.26 (m, 24H, CH$_3^{iPr}$), 1.72–1.81 (doublet-of-heptet, 2H, $^{3}J_{HH}$ = 7.1 Hz, $^{2}J_{HP}$ = 2.2 Hz, CH^{iPr}), 2.08–2.18 (overlapping doublet-of-heptet, 4H, *J* = 7.2 Hz, CH^{iPr}), 2.68 (s, 2H, NC*H*$_2$P), 2.95 (s, 4H, NC*H*$_2$P). ^{13}C{^{1}H} NMR ($CDCl_3$, 126 MHz) δ: 18.9 (s, CH$_3^{iPr}$), 19.2 (d, $^{2}J_{CP}$ = 11.1 Hz, CH$_3^{iPr}$), 19.7 (s, CH$_3^{iPr}$), 19.8 (s, CH$_3^{iPr}$), 23.0 (d, $^{1}J_{CP}$ = 12.2 Hz, CH^{iPr}), 28.6 (t, $^{1}J_{CP}$ = 11.8 Hz, CH^{iPr}), 57.4–57.8 (m, N*C*H$_2$P-coordinated), 62.6–62.9 (m, N*C*H$_2$P-uncoordinated), 203.6 (m, CO), 205.7–205.8 (m, CO). ^{31}P{^{1}H} NMR ($CDCl_3$, 162 MHz) δ: –9.22 (s, 1P, P-uncoordinated), 9.99 (s, 2P, P-coordinated) with ^{183}W satellites (d, $^{1}J_{P183W}$ = 218.3 Hz). ATR-FTIR (v/cm^{-1}): carbonyl stretches 1852, 1894, 2000. MS (ES): *m/z* 574 (100%), 576 (85%), 572 (75%), 675 (5%). Anal. calcd. for $C_{25}H_{27}NO_4P_3W$ (found): C, 44.01 (43.94); H, 3.99 (3.94); N, 2.05 (2.16).

[W(CO)$_4$(κ^2-NP$_3^{Cyp}$)] (7)

To a suspension of NP$_3^{Cyp}$ (380mg, 0.674 mmol) in DMF (15 mL) was added [W(CO)$_6$] (237 mg, 0.674 mmol) and the solution slowly heated to 155 °C (heating too rapidly causes [W(CO)$_6$] to sublime) and stirred at this temperature for 30 hours. The solvent was removed *in vacuo* and the resultant residue was dissolved in $CHCl_3$ (3 mL) and layered with methanol (7 mL). Crystals suitable for X-ray diffraction were grown over two days, which were isolated, washed with methanol (2 x 3 mL) and dried *in vacuo* (268 mg, 0.312 mmol, 46%). ^{1}H NMR ($CDCl_3$, 400 MHz) δ: 1.28–1.47 (m, 4H, CH$_2^{Cyp}$), 1.47–2.02 (m, 46H, CH$_2^{Cyp}$ and CH^{Cyp}-uncoordinated), 2.10–2.29 (m, 4H, CH^{Cyp}-coordinated), 2.72 (s, 2H, NC*H*$_2$P), 2.92 (s, 4H, NC*H*$_2$P). ^{13}C{^{1}H} NMR ($CDCl_3$, 101 MHz) δ: 26.0 (t, J_{CP} = 4.3 Hz, CH$_2^{Cyp}$), 26.1 (d, J_{CP} = 6.2 Hz, CH$_2^{Cyp}$), 26.4 (t, J_{CP} = 4.4 Hz, CH$_2^{Cyp}$), 26.5 (d, J_{CP} = 7.1 Hz, CH$_2^{Cyp}$), 29.1 (s, CH$_2^{Cyp}$), 29.7 (s, CH$_2^{Cyp}$), 30.5 (t, J_{CP} = 13.1 Hz, CH$_2^{Cyp}$), 35.4 (d, J_{CP} = 11.6 Hz, CH^{Cyp}-uncoordinated), 39.9 (t, $^{2}J_{C183W}$ = 56.2 Hz, J_{CP} = 12.5 Hz, CH^{Cyp}-coordinated), 59.2–59.6 (m, N*C*H$_2$P-coordinated), 65.1 (m, N*C*H$_2$P-uncoordinated), 203.0 (t, $^{2}J_{CP}$ = 7.1 Hz, CO^{cis}), 205.9 (t, $^{2}J_{CP}$ = 7.8 Hz, CO^{trans}). ^{31}P{^{1}H} NMR ($CDCl_3$, 162 MHz) δ: –19.3 (s, 1P, P-coordinated), 3.48 (s, 2P, P-coordinated) with ^{183}W satellites (d, $^{1}J_{P183W}$ = 222.4 Hz). ATR-FTIR (v/cm^{-1}): carbonyl stretches 1854, 1864, 1887, 2000. HRMS (ES): *m/z* found 876.3273. Anal. calcd. for $C_{37}H_{60}NO_4P_3W$ (found): C, 51.70 (51.59); H, 7.04 (6.93); N, 1.63 (1.72).

[W(CO)$_4$(κ^2*P*-{N(CH$_2$PCyp$_2$)$_2$(CH$_2$P(O)Cyp$_2$)})] (8)

In a Young's tap NMR tube, **7** was suspended in d_6-DMSO (0.7 mL) and the suspension heated to 100 °C for 10 hours, before the mixture was analyzed by ^{1}H and ^{31}P{^{1}H} NMR spectroscopy (at 100 °C to ensure the solution was homogeneous). The NMR sample was heated between 110–150 °C in 10 °C increments, for two hours at each temperature, and the formation of **8** was observed by NMR spectroscopy. Slow evaporation of the DMSO solution in air afforded pale yellow crystals suitable for X-ray diffraction. ^{31}P{^{1}H} NMR ($CDCl_3$, 162 MHz) δ: 4.69 (s) with ^{183}W satellites (d, $^1J_{P183W}$ = 221.7 Hz), 50.5 (s, P=O).

[W(CO)$_4$(κ^2*P*-PPN^{Cyh})] (10)

To a suspension of PPN^{Cyh} (1.09 g, 1.34 mmol) in DMF (15 mL) was added [W(CO)$_6$] (472 mg, 1.34 mmol) and the solution slowly heated to 110 °C (heating too rapidly causes [W(CO)$_6$] to sublime) and stirred at this temperature for 20 hours. After cooling to room temperature the solvent was removed *in vacuo* and the resultant residue dissolved in toluene and layered with methanol. Crystals suitable for X-ray diffraction grew over two days, which were isolated *via* cannula, washed with methanol (2 x 2 mL) and dried *in vacuo* (520 mg, 0.642 mmol, 48%). ^{1}H NMR ($CDCl_3$, 400 MHz) δ: 1.11–2.18 (m, 44H, Cyh), 4.16 (s, 4H, NC*H*2P), 6.58–6.64 (m, 2H, CH^{pyridyl}), 7.46–7.52 (m, 1H, CH^{pyridyl}), 8.11–8.15 (m, 1H, CH^{pyridyl}). ^{13}C{^{1}H} NMR ($CDCl_3$, 101 MHz) δ: 26.3 (s, CH$_2^{Cyh}$), 27.5 (dt, *J* = 30.3 Hz, *J* = 4.3 Hz, CH$_2^{Cyh}$), 28.7 (s, CH$_2^{Cyh}$), 29.8 (s, CH$_2^{Cyh}$), 47.6 (m, N*C*H$_2$P), 106.3 (s, CH^{pyridyl}), 113.4 (s, CH^{pyridyl}), 137.6 (s, CH^{pyridyl}), 147.7 (s, CH^{pyridyl}). ^{31}P{^{1}H} NMR ($CDCl_3$, 162 MHz) δ: 5.79 (s) with ^{183}W satellites (d, $^1J_{P183W}$ = 218.5 Hz). HRMS (ES): *m/z* calcd. for $C_{35}H_{53}N_2O_4P_2{}^{184}W$ ([M+H]$^+$) 811.2990, found 811.2979. Anal. calcd. for $C_{35}H_{52}N_2O_4P_2W$ (found): C, 51.86 (51.75); H, 6.47 (6.37); N, 3.46 (3.28).

Acknowledgements

We are grateful to Imperial College London for funding, via the Frankland Chair endowment. Dr Patricia Hunt is thanked for guidance in DFT calculations and analysis.

Notes and references

1 (a) T. J. Korstanje, J. I. van der Vlugt, C. J. Elsevier, B. de Bruin, *Science*, 2015, **350**, 298 (b) T. vom Stein, M. Meuresch, D. Limper, M. Schmitz, M. Holscher, J. Coetzee, D. J. Cole-Hamilton, J. Klankermayer, W. Leitner, *J. Am. Chem. Soc.*, 2014, **136**, 13217 (c) F. M. A. Geilen, B. Engendahl, M. Holscher, J. Klankermayer, W. Leitner, *J. Am. Chem. Soc.*, 2011, **133**, 14349 (d) X. J. Cui, Y. H. Li, C. Topf, K. Junge, M. Beller, , *Angew. Chem. Int. Ed.*, 2015, **54**, 10596 (e) Y. H. Li, C. Topf, X. J. Cui, K. Junge, M. Beller, , *Angew. Chem. Int. Ed.*, 2015, **54**, 5196

2 (a) T. vom Stein, T. den Hartog, J. Buendia, S. Stoychev, J. Mottweiler, C. Bolm, J. Klankermayer, W. Leitner, *Angew. Chem. Int. Ed.*, 2015, **54**, 5859. (b) T. vom Stein, T. Weigand, C. Merkens, J. Klankermayer, W. Leitner, *ChemCatChem*, 2013, **5**, 439.

3 K. Beydoun, T. vom Stein, J. Klankermayer, W. Leitner, , *Angew. Chem. Int. Ed.*, 2013, **52**, 9554.

4 E. J. Derrah, M. Hanauer, P. N. Plessow, M. Schelwies, M. K. da Silva, T. Schaub, *Organometallics*, 2015, **34**, 1872.

5 (a) S. Wesselbaum, V. Moha, M. Meuresch, S. Brosinski, K. M. Thenert, J. Kothe, T. V. Stein, U. Englert, M. Holscher, J. Klankermayer, W. Leitner, *Chem. Sci.*, 2015, **6**, 693 (b) S. Wesselbaum, T. vom Stein, J. Klankermayer, W. Leitner, , *Angew. Chem. Int. Ed.*, 2012, **51**, 7499.

6 A. Phanopoulos, P. W. Miller, N. J. Long, *Coord. Chem. Rev.*, 2015, **299**, 39.

7 S.-T. Liu, C.-L. Tsao, M.-C. Cheng, S. M. Peng, *Polyhedron*, 1990, **9**, 2579.

8 S. Trofimenko, *Chem. Rev.*, 1993, **93**, 943.

9 (a) F. Cecconi, S. Midollini, A. Orlandini, L. Sacconi, *Inorg. Chim. Acta.*, 1980, **42**, 59 (b) C. Bianchini, C. A. Ghilardi, A. Meli, S. Midollini, A. Orlandini, *Inorg. Chem.*, 1985, **24**, 924 (c) G. T. L. Broadwood-Strong, P. A. Chaloner, P. B. Hitchcock, *Polyhedron*, 1993, **12**, 721.

10 (a) L. Sacconi, *Coord. Chem. Rev.*, 1972, **8**, 351 (b) R. Morassi, I. Bertini, L. Sacconi, *Coord. Chem. Rev.*, 1973, **11**, 343 (c) C. Mealli, C. Ghilardi, A. Orlandini, *Coord. Chem. Rev.*, 1992, **120**, 361.

11 A.-C. Schnoor, C. Gradert, M. Schleupner, J. Krahmer, F. Tuczek, *Z. Anorg. Allg. Chem.*, 2015, **641**, 83.

12 (a) R. B. King, P. N. Kapoor, *J. Am. Chem. Soc.*, 1971, **93**, 4158 (b) C. Bianchini, E. Farnetti, M. Graziani, J. Kaspar, F. Vizza, *J. Am. Chem. Soc.*, 1993, **115**, 1753 (c) A. M. Bond, R. Colton, A. van den Bergen, J. N. Walter, *Inorg. Chem.*, 2000, **39**, 4696 (d) H. Gao, L. Chen, J. Chen, Y. Guo, D. Ye, *Catal. Sci. Technol.*, 2015, **5**, 1006.

13 (a) C. Bianchini, P. Frediani, P. Sernau, *Organometallics*, 1995, **14**, 5458 (b) C. Bianchini, A. Meli, V. Patinec, V. Sernau, F. Vizza, *J. Am. Chem. Soc.*, 1997, **119**, 4945 (c) C. Bianchini, M. Frediani, F. Vizza, *Chem. Commun.*, 2001, 479.

14 (a) P. Schober, R. Soltek, G. Huttner, L. Zsolnai, K. Heinze, *Eur. J. Inorg. Chem.*, 1998, 1407 (b) R. A. Findeis, L. H. Gade, *Dalton Trans.*, 2003, 249.

15 L. Söncksen, C. Gradert, J. Krahmer, C. Näther, F. Tuczek, *Inorg. Chem.*, 2013, **52**, 6576.

16 J. C. Peters, J. D. Feldman, T. D. Tilley, *J. Am. Chem. Soc.*, 1999, **121**, 9871.

17 (a) J. D. Feldman, J. C. Peters, T. D. Tilley, *Organometallics*, 2002, **21**, 4050 (b) M. C. Lipke, T. D. Tilley, *J. Am. Chem. Soc.*, 2011, **133**, 16374 (c) M. C. Lipke, T. D. Tilley, *Angew. Chem. Int. Ed.*, 2012, **51**, 11115 (d) M. C. Lipke, T. D. Tilley, *J. Am. Chem. Soc.*, 2013, **135**, 10298 (e) M. C. Lipke, F. Neumeyer, T. D. Tilley, *J. Am. Chem. Soc.*, 2014, **136**, 6092.

18 (a) T. A. Betley, J. C. Peters, *Inorg. Chem.*, 2003, **42**, 5074 (b) S. D. Brown, J. C. Peters, *J. Am. Chem. Soc.*, 2004, **126**, 4538 (c) C. T. Saouma, P. Müller, J. C. Peters, *J. Am. Chem. Soc.*, 2009, **131**, 10358 (d) R. A. Kinney, C. T. Saouma, J. C. Peters, B. M. Hoffman, *J. Am. Chem. Soc.*, 2012, **134**, 12637 (e) C. T. Saouma, C. C. Lu, M. W. Day, J. C. Peters, *Chem. Sci.*, 2013, **4**, 4042.

19 A. Phanopoulos, N. J. Brown, A. J. P. White, N. J. Long, P. W. Miller, *Inorg. Chem.*, 2014, **53**, 3742.

20 A. Phanopoulos, A. J. P. White, N. J. Long, P. W. Miller, *ACS Catal.*, 2015, **5**, 2500.

21 (a) W. O. Siegl, S. J. Lapporte, J. P. Collman, *Inorg. Chem.*, 1973, **12**, 674 (b) G. Kiss, I. Horváth, *Organometallics*, 1991, **10**, 3798 (c) A. B. Chaplin, P. J. Dyson, *J. Organomet. Chem.*, 2011, **696**, 2485.

22 S. J. Kyran, S. Muhammad, M. Knestrick, A. A. Bengali, D. J. Darensbourg, *Organometallics*, 2012, **31**, 3163.

23 (a) D. J. Rauscher, E. G. Thaler, J. C. Huffman, K. G. Caulton, *Organometallics*, 1991, **10**, 2209 (b) C. Landgrafe, W. S. Sheldrick, M. Südfeld, *Eur. J. Inorg. Chem.*, 1998, 407.

24 P. W. Miller, A. J. P. White, *J. Organomet. Chem.*, 2010, **695**, 1138.

25 J. L. Fillol, A. Kruckenberg, P. Scherl, H. Wadepohl, L. H. Gade, *Chem. Eur. J.*, 2011, **17**, 14047.
26 G. Märkl, G. Y. Jin, *Tetrahedron Lett.*, 1981, **22**, 1105.
27 P. Scherl, A. Kruckenberg, S. Mader, H. Wadepohl, L. H. Gade, *Organometallics*, 2012, **31**, 7024.
28 S. Dilsky, *J. Organomet. Chem.*, 2007, **692**, 2887.
29 O. Walter, S. G. Huttner, R. Kerm, *Z. Naturforsch.*, 1996, **51b**, 922.
30 A. Kütt, T. Rodima, J. Saame, E. Raamat, V. Mäemets, I. Kaljurand, I. A. Koppel, R. Y. Garlyauskayte, Y. L. Yagupolskii, L. M. Yagupolskii, E. Bernhardt, H. Willner, I. Leito, *J. Org. Chem.*, 2011, **76**, 391.
31 M. J. Hanton, S. Tin, B. J. Boardman, P. Miller, *J. Mol. Catal. A*, 2011, **346**, 70.
32 C. A. Tolman, *Chem. Rev.*, 1977, **77**, 313.
33 T. E. Müller, D. M. P. Mingos, *Transition Met. Chem.*, 1995, **20**, 533.
34 P. W. N. M. van Leeuwen, P. C. J. Kamer, J. N. H. Reek, P. Dierkes, *Chem. Rev.*, 2000, **100**, 2741.
35 N. G. Andersen, B. A. Keay, *Chem. Rev.*, 2001, **101**, 997.
36 (a) D. W. Allen, B. F. Taylor, *J. Chem. Soc., Dalton Trans.*, 1982, 51 (b) P. W. Dyer, J. Fawcett, M. J. Hanton, R. D. W. Kemmitt, R. Padda, N. Singh, *Dalton Trans.*, 2003, 104 (c) L. Tuxworth, L. Baiget, A. Phanopoulos, O. J. Metters, A. S. Batsanov, M. A. Fox, J. A. K. Howard, P. W. Dyer, *Chem. Commun.*, 2012, **48**, 10413.
37 *CRC Handbook of Chemistry and Physics*, ed. D. R. Lide, CRC Press, Taylor & Francis Group, Boca Raton, 2008-2009 Edition.